

Copyright © 1989, by the author(s).
All rights reserved.

Permission to make digital or hard copies of all or part of this work for personal or classroom use is granted without fee provided that copies are not made or distributed for profit or commercial advantage and that copies bear this notice and the full citation on the first page. To copy otherwise, to republish, to post on servers or to redistribute to lists, requires prior specific permission.

**TRAVELING-WAVE-TUBE SIMULATION;
THE IBC CODE**

by

I. J. Morey and C. K. Birdsall

Memorandum No. UCB/ERL M89/116

26 September 1989

**TRAVELING-WAVE-TUBE SIMULATION;
THE IBC CODE**

by

I. J. Morey and C. K. Birdsall

Memorandum No. UCB/ERL M89/116

26 September 1989

ELECTRONICS RESEARCH LABORATORY

College of Engineering
University of California, Berkeley
94720

TITLE PAGE

**TRAVELING-WAVE-TUBE SIMULATION;
THE IBC CODE**

by

I. J. Morey and C. K. Birdsall

Memorandum No. UCB/ERL M89/116

26 September 1989

ELECTRONICS RESEARCH LABORATORY

**College of Engineering
University of California, Berkeley
94720**

Traveling-Wave-Tube Simulation; the IBC Code

by I.J. Morey and C.K. Birdsall

ERL, University of California, Berkeley, CA 94720

Introduction

Interactive Beam-Circuit (IBC) is a one-dimensional many particle simulation code which has been developed to run interactively on a PC or Workstation, displaying most of the important physics of a traveling-wave-tube as shown in Figure 1, from Pierce 1950. The code is a substantial departure from previous efforts, since it follows all of the particles in the tube, rather than just those in one wavelength, as commonly done, for example, by Tien *et al.* (1955), Poulter (1954), and Rowe (1961). This step allows for nonperiodic inputs in time, a nonuniform line and a large set of spatial diagnostics. The primary aim is to complement a microwave tube lecture course, although past experience has shown that such codes readily become research tools.

Simple finite difference methods are used to model the fields of the coupled slow-wave transmission line. The coupling between the beam and the transmission line is based upon the finite difference equations of Brillouin (1949). The space-charge effects are included, in a manner similar to that used by Hess (1961); the original part is use the of particle-in-cell techniques (see, for example, Birdsall and Langdon, 1985) to model the space-charge fields.

1. Coupling between the Beam and the Circuit

The equations in Brillouin (1949) assume that there is strong coupling between the beam and the circuit. All the beam charge within a section of the tube induces a charge on the equivalent circuit, as shown in Figure 2 which has been taken from Brillouin.

$I_{n-1/2}$ is the current in the section between node $n-1$ and n . V_n is the voltage at node n . $L_0 = Ld_0$ and $C_0 = Cd_0$ are the self-inductance and capacitance per section Δx , and

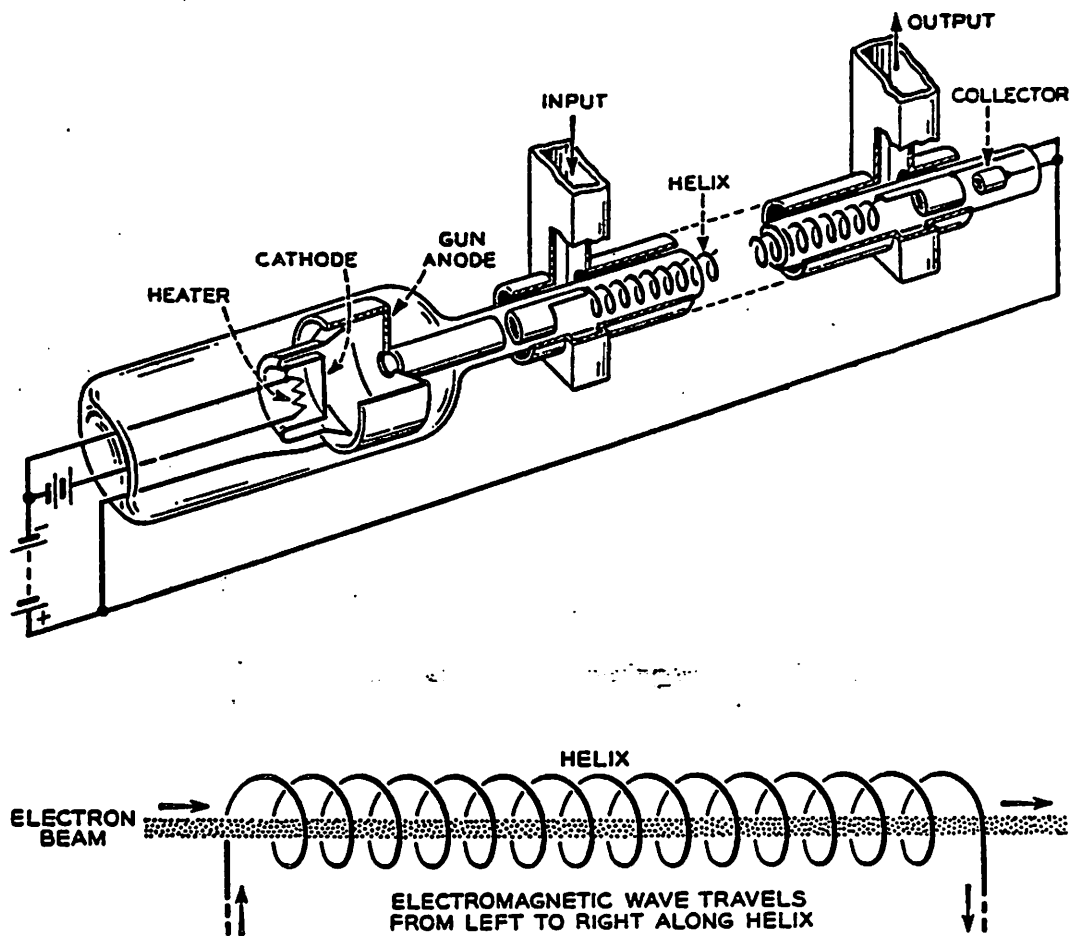


Figure 1. Schematic of a traveling-wave tube and simplified sketch of electron beam and circuit (These are Figs 2.1 and 2.2 from Pierce (1950).)

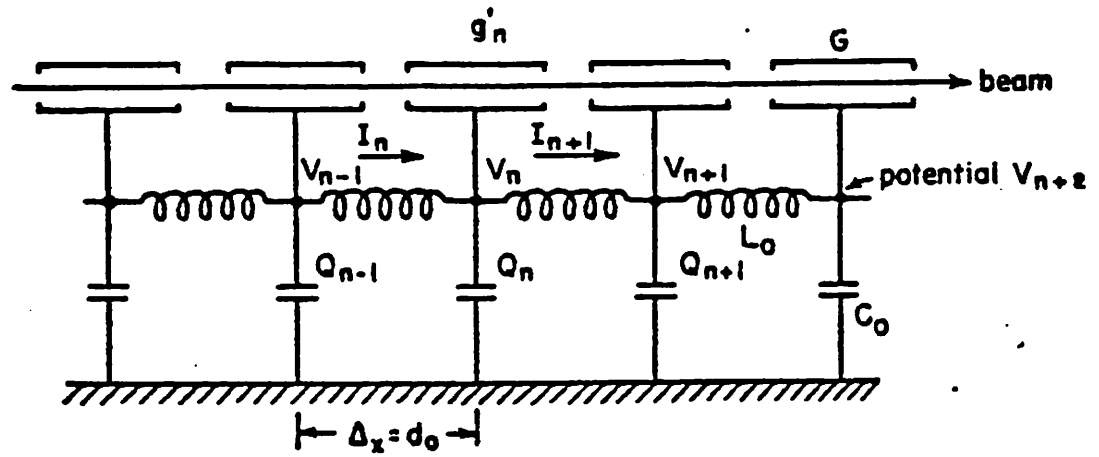


Figure 2. Transmission line model of a traveling-wave tube. (This is Fig 1. from Brillouin (1949).) Read $n-\frac{1}{2}$ and $n+\frac{1}{2}$ in place of n , $n=1$ for I, for this paper.

Q_n is the charge on the capacitor at node n , which is the sum of q_n deposited by the line and q'_n deposited by the beam.

Using the notation in Brillouin, one obtains the following space-centered equations for transmission along the line:

$$\begin{aligned} I_{n-1/2} - I_{n+1/2} &= \frac{\partial q_n}{\partial t}, & L_0 \left(\frac{\partial I_{n-1/2}}{\partial t} \right) &= V_{n-1} - V_n \\ V_n &= \frac{Q_n}{C_0}, & Q_n &= q_n + q'_n = q_n + \rho_n d_0, \end{aligned} \quad (1)$$

In IBC, however, the image charge, q'_n , is only a fraction of the beam space charge in the guiding section G , and is dependent on the wavenumber of the space-charge waves. In the IBC code we use the capacitor charge as:

$$Q_n = q_n + \kappa(k)q'_n. \quad (2)$$

The beam-circuit coupling factor $\kappa(k) \leq 1$ reflects the nature of the space-charge coupling constants for finite diameter TWTs, where beam motion produces displacement currents which induce conduction currents in the slow waveguide. The functional dependence of $\kappa(k)$ on k depends on the relative diameters of the beam and the slow waveguide, and the transverse field profiles of the different wave modes. To determine $\kappa(k)$ exactly, one would have to use complex field theory; see Birdsall and Schumacher (1959) for comments on choices for a helix.

2. Space-Charge Effects

Some of the early analytic models neglected the effects of space charge (*eg.* Nordsieck, 1953). For small wave amplitudes this neglect may be acceptable, but not so for large amplitude signals near saturation. Early space-charge models followed a wavelength of disks or rings, usually with approximate space-charge fields only. Hess (1961) calculated the effect of space-charge as another force acting on the beam electrons, effectively using a continuous beam with marker particles. The total force on the electrons is therefore a sum of the forces due to circuit fields and space-charge fields. We have adopted a similar approach, but in IBC we model the space-charge field using the more modern PIC techniques, that is, with a spatial mesh.

We assume that there is no DC space charge because the unperturbed electron beam is neutralized by co-moving or immobile ions; this assumption obviates the need to specify the focusing method of the beam (such as confined or Brillouin flow). We choose a uniform radial density profile for the beam and the ions.

We assume that the perturbed space-charge field variables (such as E_x) have a radial profile of the form $J_0(k_\perp r)$, (TM_{01}) where $k_\perp = 2.405/r_{beam}$ and r_{beam} is the beam radius. This mode implies that there is a conductor at the edge of the beam. We then use Poisson's equation for the perturbed space-charge potential, ϕ , and density, ρ , in cylindrical coordinates as

$$\frac{\partial^2 \phi}{\partial x^2} - k_\perp^2 \phi = -\frac{\rho}{\epsilon_0}, \quad (3)$$

where $\phi(x, r, \theta) = \phi(x)J_0(k_\perp r)$ and similarly for ρ . The finite difference solution to this equation using PIC techniques is discussed in the next section.

Choosing the propagation to be $\exp j(kx - \omega t)$ in Eq. 3, one obtains

$$\phi(k) = \frac{1}{\epsilon_0} \frac{1}{k^2} \left(\frac{k^2}{k^2 + k_\perp^2} \right) \rho(k). \quad (4)$$

This equation displays the usual space-charge reduction factor, where the effective plasma frequency is $\omega_q \equiv R\omega_p$,

$$R(k_\parallel, k_\perp) \equiv \left(\frac{k_\parallel^2}{k_\parallel^2 + k_\perp^2} \right)^{1/2} \leq 1 \quad (5)$$

This factor gives a simple accounting for the reduction of the axial fields and presence of transverse fields. The question of 'best' choice of k_\perp depends on the type of slow-wave circuit chosen. As noted above, we choose to use k_\perp as if the slow-wave circuit were a drift tube at the beam edge, perhaps best for coupled-cavity circuits. However, for a helix circuit, the somewhat larger reduction factor for free space may be more appropriate (Birdsall and Schumacher, 1959).

An additional feature has also been added so that the effects of space charge can be observed easily. The space-charge coupling constant $SCcoup$ allows the user to change the strength of the space-charge force. When $SCcoup = 1$, the full effect of the space charge is included, but when $SCcoup = 0$ the space-charge force has no effect; see Eq. 17.

3. The Particle-In-Cell Technique

The algorithms used in the IBC code are standard PIC algorithms. Every electron is advanced each time step using a discrete form of the equations of motion. The equations used in the code for acceleration a , velocity v and position are similar to the following:

$$\begin{aligned} \frac{dv}{dt} = a &\Rightarrow v(t_{new}) = v(t_{old}) + a_{average}\Delta t \\ \frac{dx}{dt} = v &\Rightarrow x(t_{new}) = x(t_{old}) + v_{average}\Delta t, \end{aligned} \quad (6)$$

where $t_{new} = t_{old} + \Delta t$, Δt is the period of a time step in seconds, and the subscript 'average' denotes the mean value of a variable between time t_{old} and time t_{new} . However, there are two differences between this pair of equations and the pair used in the code. Firstly, the electron velocities and positions are evaluated at different times, $\Delta t/2$ apart (the leap-frog time stepping scheme), so that $v(t_{old} + \Delta t/2)$ will approximate $v_{average}$ if Δt is sufficiently small. Similarly for $a_{average}$. Secondly, the code uses normalized units, so that $x_{code} = x/\Delta x$ and $v_{code} = v(\Delta t/\Delta x)$, where Δx is the cell width in meters ($\Delta x = \text{length of tube, } L/\text{number of cells, } N_C$). The other variables in the code are also dimensionless; for example, for the potential and the electric field, we use

$$V_{code} = V \frac{e}{m} \frac{(\Delta t)^2}{(\Delta x)^2} \quad E_{code} = E \frac{e}{m} \frac{(\Delta t)^2}{\Delta x}, \quad (7)$$

where e is the magnitude of the electron charge and m is the electron mass. The equations of motion used in the code are on the right (the $-E$ is due to $q_e = -e$):

$$\begin{aligned} v_m^{t+1/2} &= v_m^{t-1/2} - \frac{e}{m} E_m^t \frac{(\Delta t)^2}{\Delta x} \Rightarrow v_m^{t+1/2} \equiv v_m^{t-1/2} - E_m^t \\ x_m^{t+1} &= x_m^t + v_m^{t+1/2} \Delta t \Rightarrow x_m^{t+1} \equiv x_m^t + v_m^{t+1/2}, \end{aligned} \quad (8)$$

where the 'm' labels a particle and 't' labels the time step.

The electrons can be located at any point along the x-axis. However the field variables are evaluated only at discrete points on a grid. The variables are evaluated at either the boundaries or the centers of the N_C cells in the simulation. N_C may be between 50 and 400. The space charge density ρ at the *cell boundaries* is approximated by assigning the charge on each electron to the two nearest cell boundaries by linear interpolation (linear-weighting or particle-in-cell). If particle 'm' is located between the grid points 'i' and 'i+1',

then the charge on particle 'm', Q_m , will be distributed so that a charge

$$Q_i \equiv Q_m \frac{x_{i+1} - x_m}{x_{i+1} - x_i} = Q_m \frac{x_{i+1} - x_m}{\Delta x} \quad (9)$$

is assigned to the i-th grid point, and a charge

$$Q_{i+1} \equiv Q_m \frac{x_m - x_i}{\Delta x} \quad (10)$$

is assigned to the (i+1)-th grid point. This weighting is given in Figure 3. After weighting all the particles in the tube, the space charge is then normalized to the standard, or injected per Δt , number of electrons per cell, N_E . A uniform positive ion space-charge is then added to produce the net charge per unit length. Because Q_i is the charge per cell, an integration in the radial dimension is implied. Therefore, due to charge conservation, the difference in the radial density profiles of the RF and DC components of the space charge does not change Q_i .

A similar weighting method is used to approximate the beam current, I_b . Like the circuit current, I_b is obtained at the *center of each cell*, at the (i+1/2)-th grid points, and at half times $(t - 1/2)\Delta t$, same as the velocity. Each electron contributes current to the two nearest cell centers by linear interpolation. If particle 'm' is located between grid points 'i-1/2' and 'i+1/2' at time $(t - 1/2)\Delta t$, the currents due to this particle are

$$I_{b,i\pm 1/2}^{t-1/2} \equiv Q_m v_m^{t-1/2} \left[\frac{1}{2} \pm \frac{x_m^{t-1/2} - x_i}{\Delta x} \right], \quad (11)$$

where

$$x_m^{t-1/2} \equiv \frac{x_m^t + x_m^{t-1}}{2} = x_m^t - \frac{v_m^{t-1/2} \Delta t}{2}. \quad (12)$$

This weighting is given in Figure 4. After the contributions from all the electrons are accumulated, the current is then normalized to units of the injected beam current.

The space-charge potential is found by solving a tridiagonal matrix which results from the finite difference form of Eq. 3:

$$MKS: \phi_{i+1} - 2\phi_i + \phi_{i-1} - \frac{2.405^2}{r_{beam}^2} \phi_i = -\frac{\rho_{b,i}}{\epsilon_o} (\Delta x)^2 \quad (13)$$

$$Code: \phi_{i+1} - 2\phi_i + \phi_{i-1} - \frac{2.405^2}{r_b^2} \phi_i = -(\omega_0 \Delta t)^2 Q_{b,i}. \quad (14)$$

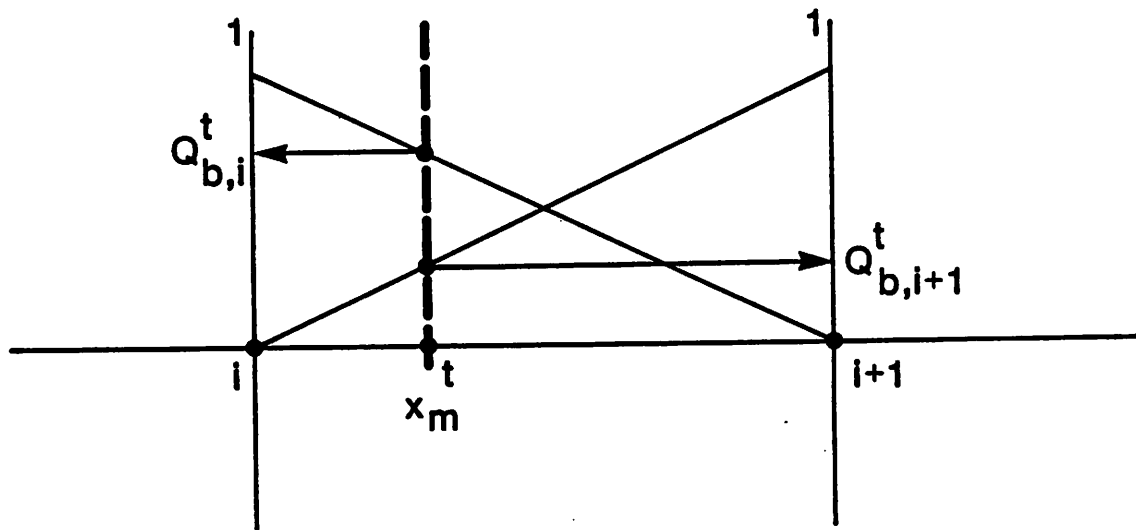


Figure 3. Beam charge weighting for particle m located between grids i and $i+1$, at time t .

A different driving term could be used due to the continuity of the beam charge,

$$\frac{\partial I_b}{\partial x} = -\frac{\partial Q_b}{\partial t}, \quad (20)$$

The option of either driving term is available in IBC. Note the similarity with Pierce's formulations as shown in his Fig 2.3, which is shown here as Figure 5.

In IBC, the telegrapher's equations have been transformed to finite-difference equations which can be solved also with leap-frog time stepping. Using the following scaling

$$I_{code} \equiv I \frac{e}{m\epsilon_0} \left(\frac{\Delta t}{\Delta x} \right)^3 \quad (21)$$

$$I_{b0} \equiv I_{beam} \frac{e}{m\epsilon_0} \left(\frac{\Delta t}{\Delta x} \right)^3 \quad (22)$$

$$Q_{b0} \equiv \frac{I_{beam}}{v_{beam}} \frac{e}{m\epsilon_0} \left(\frac{\Delta t}{\Delta x} \right)^2 \quad (23)$$

$$C_{code} \equiv C \equiv \frac{C_0}{\epsilon_0} \quad (24)$$

$$L_{code} \equiv L \equiv L_0 \epsilon_0 \left(\frac{\Delta t}{\Delta x} \right)^2, \quad (25)$$

the equations used in the code are:

$$V_i^t = V_i^{t-1} - \frac{1}{C}(I_{i+1/2}^{t-1/2} - I_{i-1/2}^{t-1/2}) + \kappa(k) \frac{Q_{b0}}{C}(Q_{b,i}^t - Q_{b,i}^{t-1}), \quad (26)$$

$$I_{i-1/2}^{t+1/2} = I_{i-1/2}^{t-1/2} - \frac{1}{L}(V_i^t - V_{i-1}^t). \quad (27)$$

Or, the other driving term could be used:

$$- \kappa \frac{I_{b0}}{C}(I_{b,i+1/2}^{t-1/2} - I_{b,i-1/2}^{t-1/2}). \quad (28)$$

The overall stencil in time and space is given in Figure 6.

The wave phase velocity, v_p , has been chosen to be $\Delta x / \Delta t$, and therefore

$$L_{code} = Z_{0code} = \epsilon_0 v_p Z_0. \quad (29)$$

The transmission line may have dispersion due to the finite differencing used. Removing the driving term from Eq. 27 and assuming propagation for V_c and I_c as $\exp j(kx - \omega t)$,

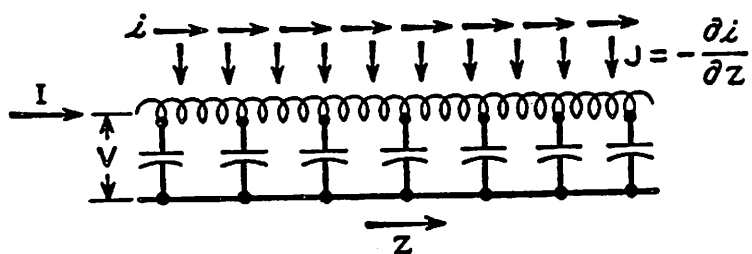


Figure 5. Transmission line model of a traveling-wave tube, with impressed beam current. (This is Fig 2.3 from Pierce (1950), with his notation.)

In the latter, $r_b = r_{beam}/\Delta x$, the subscript b in $Q_{b,i}$ signifies that it is beam space charge and not charge in the transmission line, and ω_0 is the electron plasma frequency of the beam which is determined by

$$I_{beam} = en_0 v_{beam} \pi r_{beam}^2, \quad \text{or} \quad n_0 \cong 2 \times 10^{18} \frac{I_{beam}}{v_{beam} r_{beam}^2}. \quad (15)$$

The electric field is evaluated at points in the center of each cell, offset from the space charge density and potential. Both the circuit and space-charge fields are determined by the following finite difference method:

$$E = -\nabla V \quad \Rightarrow \quad E_{i+1/2} = \frac{V_i - V_{i+1}}{\Delta x} \quad \Rightarrow \quad E_{i+1/2} = V_i - V_{i+1}, \quad (16)$$

where the last is used in the code, and similarly for ϕ , with each variable scaled appropriately. The total field is given by:

$$E_{(total)i+1/2} = E_{(circuit)i+1/2} + SCcoup * E_{(space-charge)i+1/2}. \quad (17)$$

Linear weighting is then used to obtain the field at each electron, E_m , from the two nearest cell centers, $E_{i-1/2}$ and $E_{i+1/2}$, so that

$$E_m = E_{i-1/2} \frac{x_{i+1/2} - x_m}{\Delta x} + E_{i+1/2} \frac{x_m - x_{i-1/2}}{\Delta x}. \quad (18)$$

This is the field which is used to move the electrons in the following time step.

Lastly, the boundary conditions for the particles are absorption at both the source and collector. If a particle passes the collector coordinate, for example, it is removed from the arrays which store the particle positions and velocities, and the number of electrons is decreased by one. The beam particles are injected at the source uniformly in time. Also, the space-charge potential is fixed at zero at both the source and collector.

4. The Transmission Line Algorithms

Loop and node equations may be written for the circuit in Figure 2, producing the telegraphers equations plus a driving term; in the limit of small $\Delta x, \Delta t$:

$$\begin{aligned} \frac{\partial V}{\partial t} &= -\frac{1}{C_0} \frac{\partial I}{\partial x} + \frac{1}{C_0} \frac{\partial Q_b}{\partial t}, \\ \frac{\partial I}{\partial t} &= -\frac{1}{L_0} \frac{\partial V}{\partial x} \end{aligned} \quad (19)$$

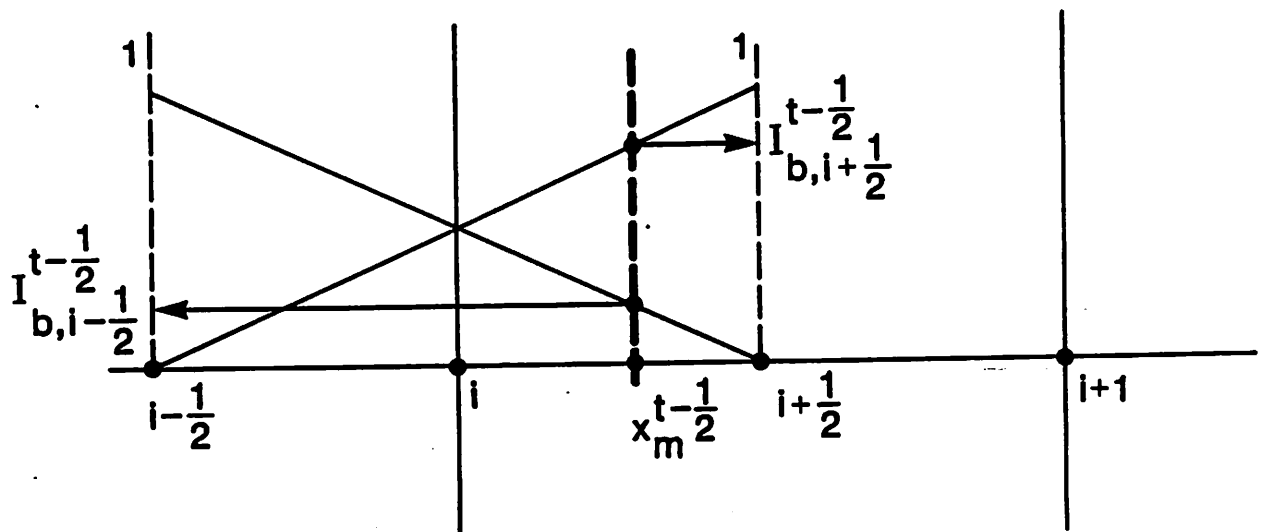


Figure 4. Beam current weighting for particle m located between grids $i-\frac{1}{2}$ and $i+\frac{1}{2}$, at time $t-\frac{1}{2}$, with velocity at time $t-\frac{1}{2}$.

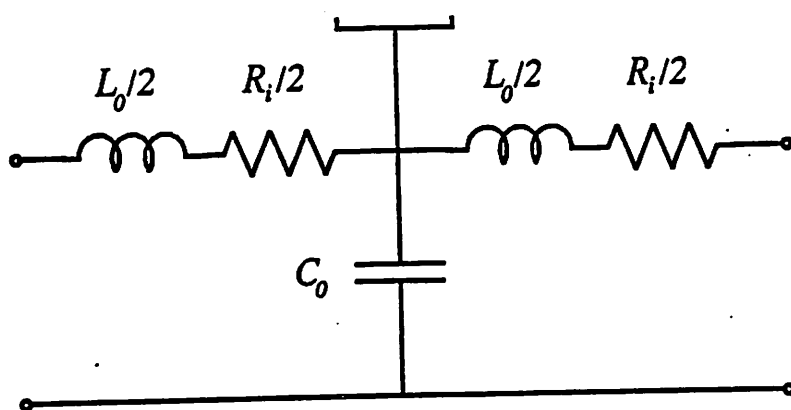


Figure 7. Addition of resistive elements to the transmission line.

at the source, and at the collector:

$$I_{N_C+1/2}^{t+1/2} = (V_{out} - V_{N_C} - (R_{out} - L)I_{N_C+1/2}^{t-1/2})(R_{out} + L)^{-1}, \quad (37)$$

where $R_{in} = \varepsilon_0 v_{phase} R_{input}$ and $R_{out} = \varepsilon_0 v_{phase} R_{output}$.

However, these terminations are matched (reflectionless) only when there is no beam-circuit coupling. The greater the coupling between the beam and the circuit, the greater the reflected signal, which can make the loop gain exceed unity, and the tube will become an oscillator. To avoid self-oscillation, a section of the transmission line is made lossy using the circuit segment shown in Figure 7.

Two options have been included in the code. The first option has a lossy section located about the center of the line, beginning at grid point N_0 , with the spatial variation of the resistance having the form:

$$R_i = R_0(1 - \cos\theta), \text{ where } \theta = 2\pi \frac{i - N_0}{N_C - 2N_0} : N_0 < i < N_C - N_0 \quad (38)$$

This loss is introduced to attenuate the reflected signal before it reaches the input end of the tube, while reducing the gain by a smaller amount (Pierce, 1950). The wave reflected from the collector end of the tube (which may be as large as 10 per cent of the incident signal) becomes larger relative to the forward (growing) wave as the reflected wave approaches the lossy section; the two waves produce an interesting interference pattern in the lossy section.

To overcome these limitations, a terminating section has been designed which is nearly fully absorbing, or reflectionless. This termination is a lossy section of line at the end of the tube, of length N_1 cells, with

$$R_i = R_t((1 + \gamma)^{i - N_C + N_1} - 1), \text{ where } R_t \leq 10^{-5} \text{ and } \gamma \leq 0.2 : i > N_C - N_1. \quad (39)$$

The coupling between the beam and the circuit has also been reduced in a tapered fashion in this section. It is not desirable to abruptly end the coupling between the beam and the circuit because this will also introduce reflections. The present loss tapering has the form:

$$\cos(2\pi(i - N_C + N_1)/4N_1), \quad (40)$$

where $x = i\Delta x$ and $t = n\Delta t$, Eq. 25 and 26 become

$$\Omega V_c = \frac{K}{C} I_c \quad (30)$$

$$\Omega I_c = \frac{K}{L} V_c. \quad (31)$$

where $\Omega = \omega \text{sinc}(\omega\Delta t/2)$ and $K = k \text{sinc}(k\Delta x/2)$ ($\text{sinc} y \equiv \sin y/y$). Eliminating V_c and I_c produces the transmission line dispersion relation

$$K^2 = \Omega^2 LC. \quad (32)$$

This equation displays two results. First, rewrite it as

$$\sin^2(\omega\Delta t/2) = \frac{\Delta t^2}{LC\Delta x^2} \sin^2(k\Delta x/2). \quad (33)$$

The right hand side must be less than one for ω to be real; hence, for a stable solution we must have

$$\Delta t \leq (LC)^{1/2} \Delta x, \quad (34)$$

a Courant condition. Second, rewrite Eq. (31) as

$$v_p^2 \equiv \frac{\omega^2}{k^2} = \frac{1}{LC} \frac{\text{sinc}^2(\omega\Delta t/2)}{\text{sinc}^2(k\Delta x/2)}. \quad (35)$$

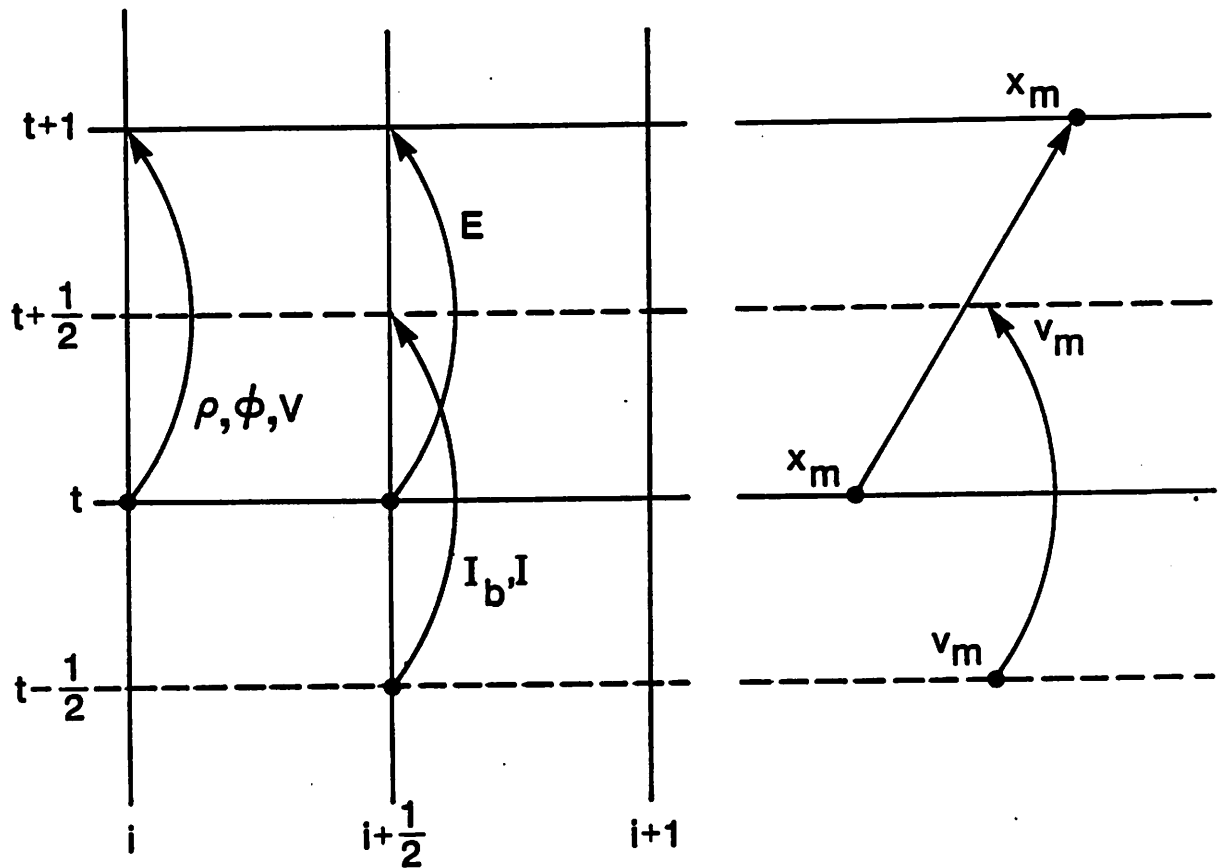
This shows that $v_p = (LC)^{-1/2}$ only when $v_p = \Delta x/\Delta t$, as used here (See Birdsall and Langdon, 1985, Section 15-3 for more discussion).

Terminations and Transmission Line Loss

The transmission line is terminated at each end with a resistor and a voltage source. Since the input and output source voltages, V_{input} and V_{output} respectively, are user defined functions of time, only the updated circuit current needs to be calculated. The passive elements terminating the transmission line are the resistors R_{input} and R_{output} , at the input and output respectively, each in series with an inductance $L_0/2$.

The resulting equations for the end half sections, in the units of the code, are:

$$I_{-1/2}^{t+1/2} = (V_{\text{in}} - V_0 - (R_{\text{in}} - L)I_{-1/2}^{t-1/2})(R_{\text{in}} + L)^{-1} \quad (36)$$



GRID QUANTITY ADVANCE

PARTICLE ADVANCE

Figure 6. Time-space stencil for both grid quantity and particle advances.

i.e., one quarter of a sinusoid. However, with $N_c = 200$ a gain of about 40dB is the maximum attainable before the reflected signal becomes comparable to the input signal. Typical parameter values used are $N_1 = 50-100$, $R_t = 10^{-6}$ and $\gamma = 0.1$.

Spatial Smoothing

Either driving term, $\partial Q_b/\partial t$ or $\partial I_b/\partial x$, produces large potential oscillations at electron bunches, which in turn cause further bunching. The driving term is spatially smoothed, with high wavenumber modes highly attenuated, representing the wavenumber dependence of the coupling coefficient, $\kappa(k)$. Actually, in IBC, $\kappa(k)$ is represented by the product of a constant, $BCcoup$, and a wavenumber filter. Any type of filter may be implemented. A Butterworth filter of order 2 is currently used,

$$\kappa(k) = \frac{BCcoup}{1 + (k/k_{max})^4}, \quad (41)$$

where k_{max} is an input parameter. This filter was chosen because it is easy to evaluate the attenuation for different k/k_{max} . If a sharper roll off is needed, a Butterworth filter of higher order could be used. If the driving term is not spatially filtered, then the simulation becomes unstable because the electrons collect in potential oscillations with a wavelength of $2\Delta x$.

The circuit voltage must also be filtered, as well as the driving term, since any short wavelength perturbation in the circuit voltage will not be damped otherwise. A digital smoothing routine (Appendix C in Birdsall and Langdon, 1985) has been added to filter the circuit voltage of high frequency components. The filter makes the following replacement:

$$V_i = \frac{WV_{i-1} + V_i + WV_{i+1}}{1 + 2W}, \quad (42)$$

first smoothing with $W = 1/2$, followed by $W = -1/6$ for small k compensation. These two steps can be repeated a number of times to further attenuate the higher frequencies.

This method is used because it does not require much CPU time. However, even the desired voltage at the longer wavelengths is attenuated by this method; that is, smoothing effectively introduces some loss in the transmission line. This is because the wave amplitude is reduced each time step as the wave moves along the transmission line. In k space, if the

circuit voltage varies sinusoidally,

$$V_{filtered}(k) = \frac{1 + 2W \cos(k\Delta x)}{1 + 2W} V(k). \quad (43)$$

Therefore, the attenuation due to the $W = 1/2$ and $W = -1/6$ filters in series is:

$$A = \frac{3}{4} - \frac{1}{2} \cos(k\Delta x) + \frac{1}{4} \cos^2(k\Delta x). \quad (44)$$

If $\lambda = 20\Delta x$, $k\Delta x = \pi/10$, then $A = 0.9994$. Since the wave velocity has been chosen to be $\Delta x/\Delta t$, the wave amplitude will be attenuated by 0.9994 each time the wave moves one cell. If this digital filtering sequence is repeated each time step $N_{smooth} V_c$ times, the wave amplitude will be attenuated by $0.9994^{N_{smooth} V_c}$ per cell. With $\lambda = 20\Delta x$, $N_{smooth} V_c = 5$ and $N_C = 100$, the attenuation along the transmission line will be:

$$V_{N_C} = 0.9994^{5 \times 100} V_0 \quad \equiv -2.6 \text{dB}. \quad (45)$$

This apparently innocent smoothing has been measured, confirming this estimate.

5. Comparison with the Dispersion Relation of Pierce; Identification of Pierce's C and QC

We have drawn heavily on the modeling used by J.R. Pierce in his book (1950) starting from the elementary model in Chapter 1 and then going on to the model which adds space-charge effects in Chapter 7. Pierce derived the following linearized relationship between the voltage at the beam, V_T , and the space charge per unit length, ρ , (his Eq. 7.7)

$$V_T = \left[\frac{\omega \beta_1 (E^2 / 2\beta^2 P)}{(\beta_1^2 - \beta^2)} + \frac{1}{C_1} \right] \rho. \quad (46)$$

The first term on the right hand side represents only the synchronous components and the asynchronous components contribute to the space-charge term, represented by the capacitance C_1 . See Figure 8 (from Pierce, 1950, his Fig 7.1). In our terminology, $\beta_1 = \omega/v_p = \omega(L_0 C_0)^{1/2}$, $\beta = -k$ and $Z_0 = E^2 / 2\beta^2 P = (L_0 / C_0)^{1/2}$, hence Pierce's equation can be transformed to

$$V_T = \left[\frac{\omega^2}{(\omega^2 - k^2 v_p^2)} \frac{1}{C_0} + \frac{1}{C_1} \right] \rho. \quad (47)$$

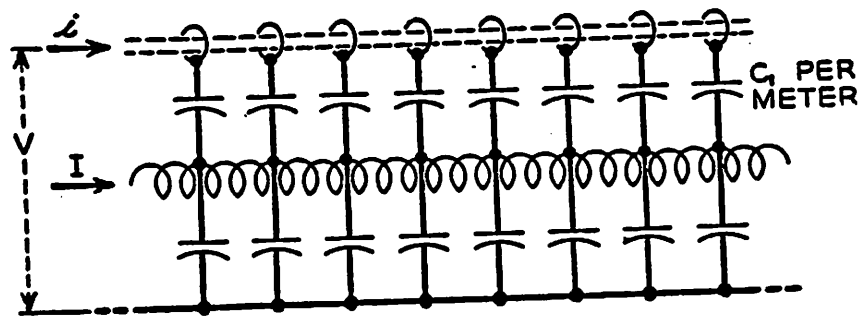


Figure 8. Transmission line model of a traveling-wave tube, with capacitors C_1 , modeling space charge. (This is Fig 7.1 from Pierce (1950).)

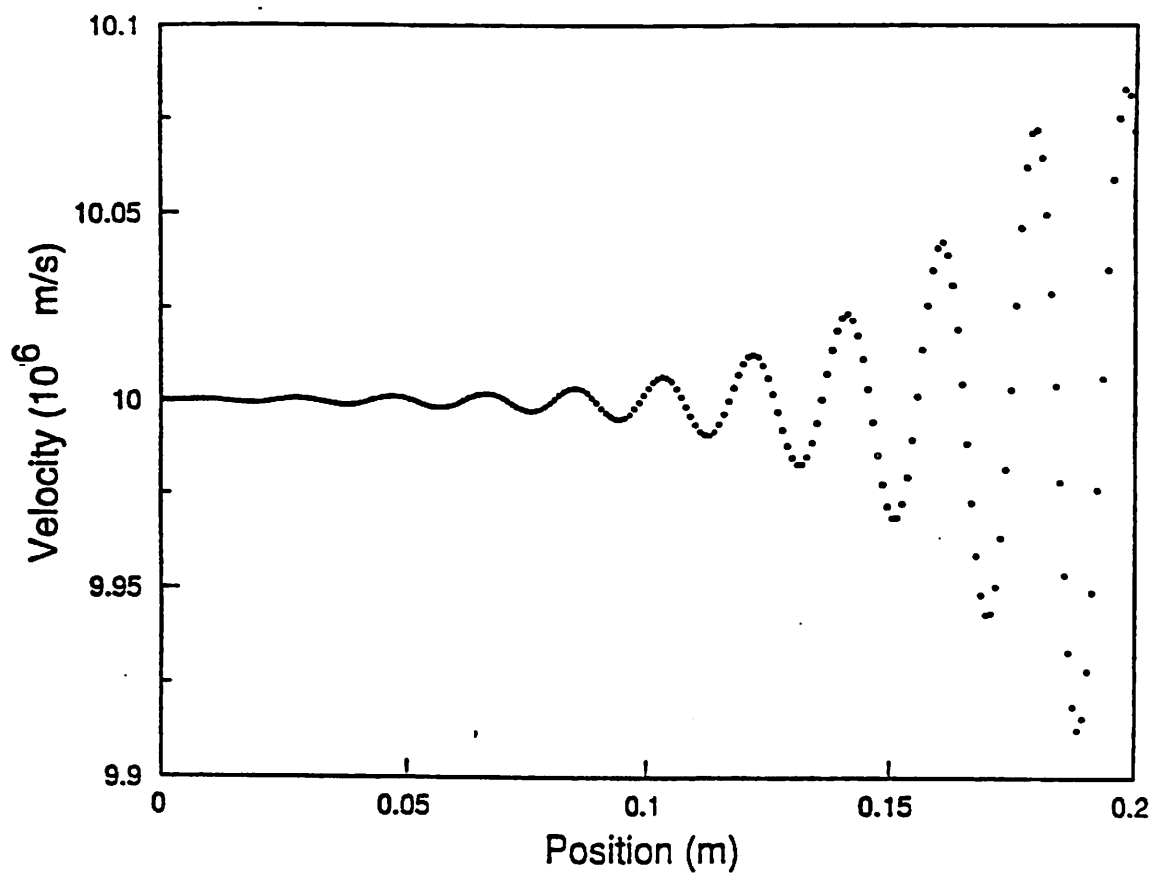


Figure 9. IBC simulation velocity-position plot (phase-space) or snapshot for the parameters given in the text. The velocity units are 10^6 m/s.

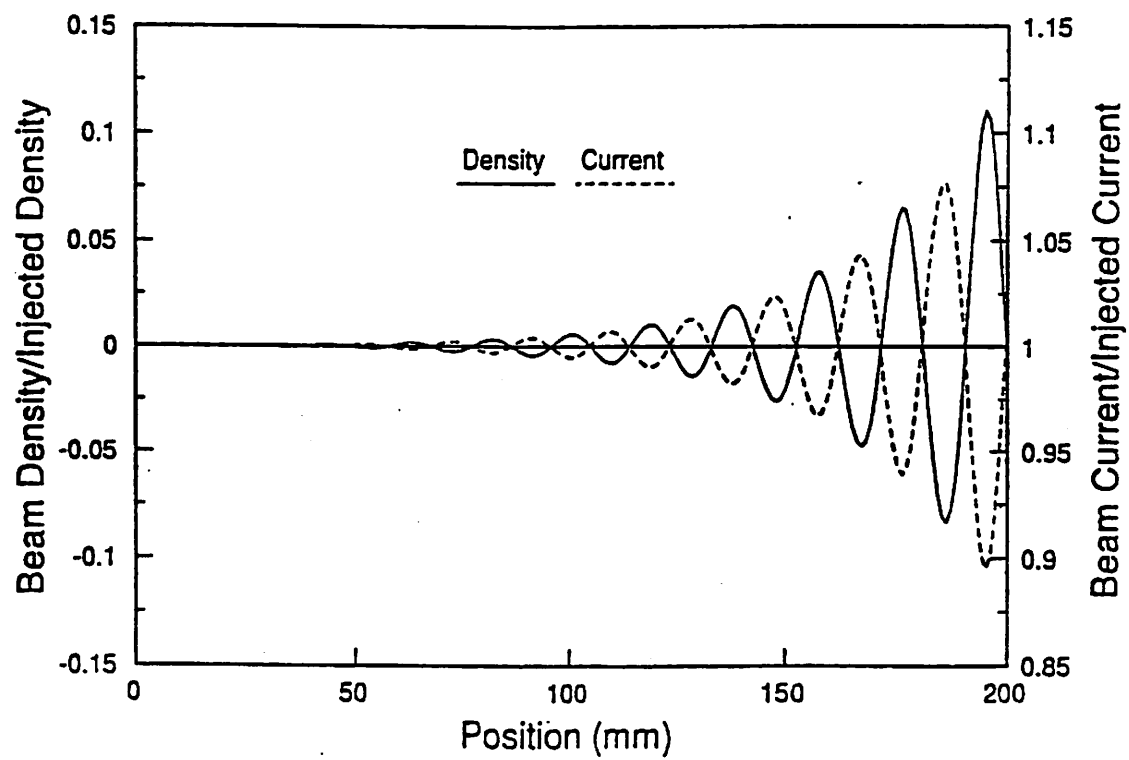


Figure 10. IBC simulation of beam charge density and current as a function of position, to go with Figure 9.

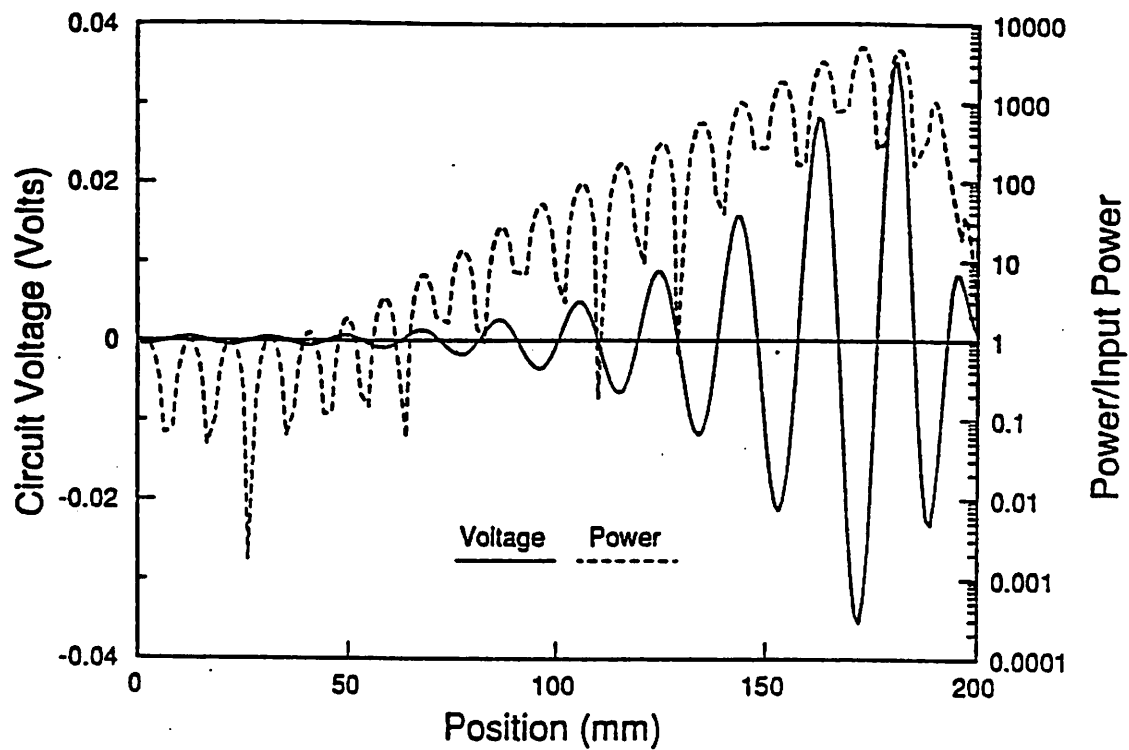


Figure 11. IBC simulation of circuit voltage and circuit power along the traveling-wave tube; to go with Figures 9 and 10. The latter is on a log scale, so that this scale may be read as 0, 10dB, 20dB, 30dB, 40dB. The tube is terminated in a tapered lossy region (as described in the text) starting at position 150mm. Hence, the peaks in voltage and power are due to absorption of the power and not due to saturation of the beam.

In our model (very much like Pierce's Fig. 2.3) we simply add the circuit voltage and that due to space-charge. We use our differential equations, linearized, to obtain

$$V_T = \left[\frac{\kappa(k)\omega^2}{(\omega^2 - k^2 v_p^2)} \frac{1}{C_0} + \frac{SCcoup R^2(k)}{\epsilon_0 k^2 A} \right] \rho, \quad (48)$$

where $\kappa(k)$ is a variable coupling between the beam and the circuit, $A = \pi r_{beam}^2$ and $R(k)$ is the reduction factor, $R = k^2/(k^2 + k_\perp^2)$. Thus we have a one-to-one correspondence to Pierce's parameters, as follows:

	Pierce	Morey and Birdsall
Circuit phase	β_1	$\frac{\omega}{v_p} = \omega(L_0 C_0)^{1/2}$
Net phase	β	$-k$
Circuit impedance	$\frac{E^2}{2\beta^2 P}$	$Z_0 = \left(\frac{L_0}{C_0}\right)^{1/2}$
Capacitance/meter term	$\frac{1}{C_0} = \left(\frac{E^2}{2\beta^2 P}\right) v_p$	$\frac{\kappa(k)}{C_0} = \kappa(k) Z_0 v_p$
Space-charge term	$\frac{1}{C_1}$	$\frac{SCcoup R^2(k)}{\epsilon_0 k^2 A}$
Gain Parameter	$C^3 = \left(\frac{E^2}{2\beta^2 P}\right) \left(\frac{I_0}{4V_0}\right)$	$Z_0 \left(\frac{I_0}{4V_0}\right) \kappa(k)$
Space-charge parameter	$Q \equiv \frac{\omega/v_p}{2\omega C_1 (E^2/2\beta^2 P)}$	$\frac{\omega/v_p SCcoup R^2(k)}{2\omega \epsilon_0 k^2 A}$
Effective plasma frequency, slower space-charge wave	$(4QC^3)^{1/2} = \frac{\omega_q/\omega}{1 + \omega_q/\omega} \approx \frac{\omega_q}{\omega}$	$\omega_q \equiv R(k)\omega_p$
Circuit loss, attenuation	$Re\Gamma_1 = \frac{\omega}{v_e} C d$	$\alpha = \frac{R_0}{2Z_0}$

In order to use the well known solutions to Pierce's small signal dispersion relation (see Birdsall and Brewer, 1954; Brewer and Birdsall, 1957), it is suggested that one start from the physical model desired and obtain Pierce's circuit impedance (same as our Z_0), then Pierce's gain parameter C^3 and C . Next, obtain Pierce's QC from ω_q/ω and Pierce's loss term d . Then, in a parallel manner, obtain the equivalent terms in our relation, also starting from the physical model; use the coupling (smoothing) term $\kappa(k)$ equal to one and the space-charge coupling term $SCcoup$ also equal to one. Then compare to make sure that the C , QC and d obtained are the same. In this manner, the Pierce growth rates and

initial loss parameter may be found and used to predict (confirm) the simulation results for small signals.

Some Typical Results

When the code is run on an IBM PS2/80, with 100-200 cells and up to 5 particles per cell, many different features of a TWT interaction can be observed in a one hour session. Quantities such as: the beam density and current, the two driving terms, the circuit voltage and current and the power, can be displayed individually or all together. Figures 9,10 and 11 show the output for a tube of length 0.2 meters, a gain of $C = 0.056$ and an absorbing termination.

The wave amplitude has saturated within the absorbing termination, because the line is very lossy. The absorbing termination is located in the final quarter of the tube. At the end of the tube the beam and circuit are decoupled and the circuit loss is 4 Ohm/meter. The greatest mismatch is at this point but the signal amplitude is only a few times that at the input end. Any reflected signal is attenuated within the last few centimeters of the tube. If the lossless region of the tube were made longer, the reflected wave amplitude would not be attenuated below the input signal amplitude.

The following input parameters were used: Length = 0.2 m, $V_{beam} = 10^7$ m/s, $V_{phase} = 10^7$ m/s, $I_{beam} = 10$ mAmps, $r_{beam} = 1$ mm, Freq = 500 MHz, $Z_o = 20$ Ohms, $R_{in} = 20$ Ohms, $R_{out} = 20$ Ohms, $V_{in} = 1$ mVolt, $R_t = 10^{-5}$, $\gamma = 0.18$, $N_1 = 50$, $N_C = 200$, $N_E = 1$, $BC_{coup} = 1.0$, $SC_{coup} = 1.0$, $k_{max} = 2k_0$, $N_{smoothVc} = 1$ and the driving term was $\partial\rho/\partial t$.

Acknowledgments

This work was supported in part by a UCLA sub-contract from Rome Air Development Center, Air Force Contract F30602-87-0201.

References

- C.K. Birdsall and G.R. Brewer, "Traveling wave tube characteristics for finite values of C ", IRE Trans. PGED, ED-1, pp. 1-11, August 1954.
- C.K. Birdsall and A.B. Langdon, *Plasma Physics via Computer Simulation*, McGraw Hill, New York, 1985.
- C.K. Birdsall and F.M. Schumacher, "Plasma frequency reduction in electron streams by helices and drift tubes", IRE Trans. PGED, ED-6, October 1959.
- G.R. Brewer and C.K. Birdsall, "Traveling-wave tube propagation constants", IRE Trans. PGED, ED-4, pp. 140-144, April 1957.
- L. Brillouin, "The traveling-wave tube (discussion of waves for large amplitudes)", J. App. Phys., 20, pp. 1196-1206, December 1949.
- R.L. Hess, "Large-signal traveling wave tube operation: concepts and analysis", USAF Aeronautical Systems Division Technical Report 61-15, July 1961. Also, Ph.D. thesis, May 1960, University of California, Berkeley, CA 94720.
- A. Nordsieck, "Theory of the large-signal behavior of traveling-wave amplifiers", Proc. IRE, 41, pp. 630-637, May 1953.
- J.R. Pierce, *Traveling Wave Tubes*, D. Van Nostrand, New York, 1950.
- H.C. Poulter, "Large signal theory of the traveling-wave tube", Tech. Rep. 73, ERL, Stanford University, January 1954.
- J.E. Rowe, "A large-signal analysis of the traveling-wave amplifier: Theory and results", PGED ED-3, pp. 39-56, January 1956
- P.K. Tien, L.R. Walker and V.M. Wolontis, "A large-signal theory of traveling-wave amplifier", Proc. IRE, 43, pp. 260-277, March 1955.

Figure Captions

Figure 1. Schematic of a traveling-wave tube and simplified sketch of electron beam and circuit (These are Figs 2.1 and 2.2 from Pierce (1950).)

Figure 2. Transmission line model of a traveling-wave tube. (This is Fig 1. from Brillouin (1949).) Read $n-1/2$ and $n+1/2$ in place of n , $n=1$ for I, for this paper.

Figure 3. Beam charge weighting for particle m located between grids i and $i+1$, at time t .

Figure 4. Beam current weighting for particle m located between grids $i-1/2$ and $i+1/2$, at time $t-1/2$, with velocity at time $t-1/2$.

Figure 5. Transmission line model of a traveling-wave tube, with impressed beam current. (This is Fig 2.3 from Pierce (1950), with his notation.)

Figure 6. Time-space stencil for both grid quantity and particle advances.

Figure 7. Addition of resistive elements to the transmission line.

Figure 8. Transmission line model of a traveling-wave tube, with capacitors C_1 , modeling space charge. (This is Fig 7.1 from Pierce (1950).)

Figure 9. IBC simulation velocity-position plot (phase-space) or snapshot for the parameters given in the text. The velocity units are 10^6 m/s.

Figure 10. IBC simulation of beam charge density and current as a function of position, to go with Figure 9.

Figure 11. IBC simulation of circuit voltage and circuit power along the traveling-wave tube; to go with Figures 9 and 10. The latter is on a log scale, so that this scale may be read as 0, 10dB, 20dB, 30dB, 40dB. The tube is terminated in a tapered lossy region (as described in the text) starting at position 150mm. Hence, the peaks in voltage and power are due to absorption of the power and not due to saturation of the beam.

The following appendices provide detailed instructions on running the IBC program on a personal computer. For more instructions on obtaining copies of the code, write to Prof. C.K. Birdsall.

Appendix I: Disk Contents

The IBC disk contains the following files:

IBC.EXE IBC executable file. This file must be in the current directory or on the current path to run IBC. See your DOS manual for information on paths and directories.

***.INP** All files with the INP extension are the input decks.

***.C** All files with the C extension are the C language source files for the IBC. These are:

IBC.C contains the `main()`, heart of IBC, from which all the other routines are called in the sequence explained in the next section.

INIT.C contains the function `init()`.

MOVE.C contains the function `move()`.

DRIVE.C contains the function `drive()`.

CIRCUIT.C contains the function `circuit()`.

FIELD.C contains the function `field()`.

PLOT.C contains the functions `selectplot()`, `screen()`, `plotall()`, `plotpoint()` and `plotline()`.

SWITCH.C contains the function `ChangeAndDisplayParam()`.

FFT.C contains the FFT routines used in one the filters.

IBC.H The C language header file for IBC.

***.OBJ** All files with this extension are the object files for IBC. These are provided for users who wish to extend some parts of the code but are using a compiler other than Microsoft C 5.

IBC.MAK The MAKE utility file for automatically performing conditional compilation/linking of only those files which have been changed. Requires the Microsoft MAKE utility provided with many recent compilers (including C 5, Quick C 1, FORTRAN 4, and MASM 5).

Appendix II: Sequence of steps in IBC

Since it is expected that users will modify and improve this code a brief description of steps in the program and the functions called is provided here.

A) The function init() is called to:

- i) Load default values of the code parameters.**
- ii) Read in new parameters from an input deck (if no input deck is provided read IBC.INP).**
- iii) Check for inappropriate input parameters and warn the user.**
- iv) Scale parameters to normalized code units.**
- v) Initialize other variables (no current or voltage in the circuit, no field at the beam and the beam is already across the tube).**

B) Start of time stepping loop.

C) The function move() is called to:

- i) Move beam electrons.**
- ii) Remove beam electrons which reach the collector.**
- iii) Inject more beam electrons.**
- iv) Calculate beam density.**
- v) Calculate beam current.**

D) Switch for changing and displaying some of the parameters if the user requests.

E) The function drive() is called to Filter driving term.

F) The function circuit() is called to:

- i) Update circuit voltage(some smoothing is included).**
- ii) Update circuit current.**

G) The function field() is called to:

- i) Calculate space-charge potential.**
- ii) Add circuit and space-charge fields to get total field.**
- iii) Interpolate field at grid points to each beam electron.**

H) Switch for changing and displaying some of the parameters if the user requests.

I) The function SelectPlot() is called to display graphics.

J) End of time stepping loop.

Appendix III: Running the IBC Code

To run IBC code type IBC [*filename.ext*], where *filename.ext* is the name of an input file (although we have used *xxxxx.INP*, the *.INP* extension is not required). If no file name is provided on the command line, IBC looks for a file named *IBC.INP*. However, if this file cannot be read then the default values, which are loaded in the main program, will be used. Once this is done, all the input parameters are displayed in MKS units in the following format:

Length (m)	Beam Velocity (m/s)	Wave Velocity (m/s)	
Frequency (Hz)	Beam Current (Amps)	Beam Radius (m)	
Z_0 (Ohm)	R_{in} (Ohm)	R_{out} (Ohm)	V_{in} (Volts)
R_0 (Ohm/m)	n_0	γ	n_1
L_0 (Henry/m)	C_0 (Farad/m)	N_0 (electron/m ³)	W_0 (Hz)
Wavelength (m)	Mode (Length/Wavelength)		
k_{max}/k_0	$N_{smoothDr}$	$N_{smoothVc}$	
nc	$nfft$	ne	
BCcoup	SCcoup		

A warning message may also appear with the above display if an input parameter is outside of an acceptable range. This is to guide users of the code who are unfamiliar with the PIC technique or TWTs. The input parameters can be changed by editing the input file, although this may not be necessary since many can be changed while the program is running.

Following this display some code parameters are listed. This list was used as a diagnostic during the initial stages of development, and still provide some useful information.

At the start of the simulation a list of options will appear on the screen. It tells the user which keys to press to select which variables will be displayed graphically. These keys are:

a - plot all diagnostics

v - plot electron velocities

q - plot electron charge density

j - plot electron beam current

d - plot the driving term

f - plot the filtered driving term

V - plot circuit voltage

e - plot circuit electric field

s - plot space-charge field

C - plot circuit current

p - plot power

l - plot circuit loss

D - display the values of some parameters

W - write variables to an output file IBC.OUT

c - change some parameters

h - returns you to this display

The **h** key will cause the simulation to pause and display the above list. The **D** key will also halt the simulation, but the parameter list, shown above, will be displayed. The **c** key displays the list of changeable parameters. This list includes:

d - changes the driving term ($d\rho/dt - dI_b/dx$)

f - changes the filter (fourier - digital)

b - changes the Beam-Circuit coupling coefficient

s - changes the Space-Charge force coefficient

n - changes the Number of loops in the Drive digital filter

N - changes the Number of loops in the Voltage digital filter

k - changes 'kmax' in the fourier filter

R - changes the beam radius

i - changes the input resistance, R_{in}

o - changes the output resistance, R_{out}

r - changes the circuit resistance, R_0

g - changes gamma in the reflectionless termination

P - changes the input voltage, V_{in}

v - changes the scale of the velocity display

q - changes the scale of the density display

j - changes the scale of the beam current display

V - changes the scale of the circuit voltage displays

e - changes the scale of the field displays

C - changes the scale of the circuit current displays

p - changes the scale of the power display

l - changes the scale of the circuit loss display

When this list is displayed, the code is actually waiting for a parameter to be selected. If you do not wish to change the value of any parameter, press a key which is not on the list to return to the previous display. When a parameter is selected the user must choose a factor by which the selected parameter can be changed, either multiply or divide. The user is given a second chance if some characters are typed in accidentally. After entering the factor, press the key '/' if division is wanted, or any other key if multiplication is desired. The new value of this parameter will then be printed on the screen. To return to the simulation at this point, just press any key.